



Pergamon

Origin of the Stereospecificity in Binding Hydroxamates of α - and β -Phenylalanine Methylamide to Thermolysin Revealed by the X-ray Crystallographic Study

Seung-Jun Kim,^a Dong H. Kim,^{b,*} Jung Dae Park,^b
Joo-Rang Woo,^a Yonghao Jin^b and Seong Eon Ryu^{a,*}

^aCenter for Cellular Switch Protein Structure, Korea Research Institute of Bioscience and Biotechnology,
52 Euh-eun-dong, Yusong-gu, Daejeon 305-806, South Korea

^bCenter for Integrated Molecular Systems, Division of Molecular and Life Sciences,
Pohang University of Science and Technology, San 31Hyoja-dong, Namku, Pohang 790-784, South Korea

Received 20 December 2002; accepted 25 February 2003

Abstract—Optically active *N*-formyl-*N*-hydroxy- α -phenylalanine methylamide (**1**) and *N*-formyl-*N*-hydroxy- β -phenylalanine methylamide (**2**) were evaluated as inhibitors for thermolysin (TLN) to find that while the *D*-form is more potent than its enantiomer in the case of the hydroxamate of α -Phe-NHMe, in the inhibition with hydroxamate of β -Phe-NHMe, the *L*-isomer ($K_i = 1.66 \pm 0.05 \mu\text{M}$) is more effective than its enantiomer. In order to shed light on the stereochemical preference observed in the inhibitions, X-ray crystallographic analyses of the crystalline TLN·*D*-**1** and TLN·*L*-**2** complexes were performed to the resolution of 2.1 Å. While *L*-**2** binds TLN like substrate does with its benzyl aromatic ring occupying the S_1' pocket, the electron density in the S_1' pocket in the complex of TLN·*D*-**1** is weak and could best be accounted for by the methylcarbamoyl moiety. For both inhibitors, the hydroxamate moiety coordinates the active site zinc ion in a bidentate fashion.

© 2003 Elsevier Science Ltd. All rights reserved.

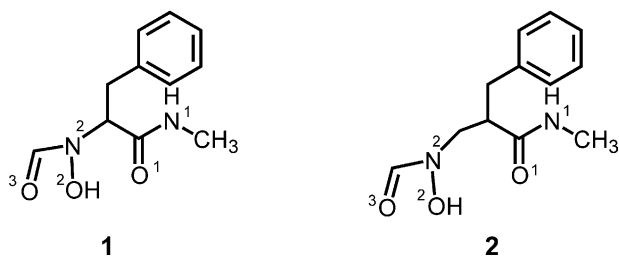
Introduction

Thermolysin (TLN) is a heat-stable proteolytic enzyme isolated from *Bacillus thermoproteolyticus* and carries a catalytically essential zinc ion at the active site.¹ The enzyme is an extracellular endopeptidase, hydrolyzing the peptide bond on the imino side of the amino acid residue having a large hydrophobic side chain, such as Leu, Ile, and Phe.¹ The enzyme has been extensively studied as a prototypical zinc enzyme and used as a model target enzyme for developing design strategies of enzyme inhibitors that can be transferred to zinc proteases of medicinal interest such as angiotensin converting enzyme² and matrix metalloproteases.³ Inhibitors of angiotensin converting enzyme are clinically important as antihypertensive agents,² and numerous inhibitors of matrix metalloproteases are presently under various stages of clinical investigations as potential antitumor and antiarthritis agents.³

Most of small molecule inhibitors for zinc proteases carry a functional group that ligates the active site zinc ion, such as carboxylate, thiol, or hydroxamate.⁴ Of these zinc ligating groups, hydroxamate occupies a prominent position because of its strong chelating property toward zinc ion.⁵ Recently, Jin and Kim reported that *N*-formyl-*N*-hydroxy-LeuOMe is a potent inhibitor for TLN but surprisingly its inhibitory activity ($K_i = 44 \mu\text{M}$) was found to be mostly vested with the *D*-isomer.⁶ Subsequently, they noted that *N*-formyl-*N*-hydroxy derivative of β -PheNHMe is even more potent but the inhibition stereochemistry is reversed compared with that of the corresponding hydroxamate of α -amino acid.⁷ Thus, the K_i value for the *L*-enantiomer of *N*-formyl-*N*-hydroxy- β -PheNHMe was shown to be 1.66 μM , but that for its enantiomer that is, *N*-formyl-*N*-hydroxy- β -*D*-PheNHMe was 68.2 μM . In order to shed light on the origin of the observed stereochemical preference in the binding of these inhibitors to TLN, we have synthesized hydroxamates of α - and β -PheNHMe (**1** and **2**) in an optically pure form, and undertaken X-ray crystallographic structure determina-

*Corresponding author. Tel.: +82-54-279-2101; fax: +82-54-279-5877;
e-mail: dhkim@postech.ac.kr (D.H. Kim); ryuse@mail.krib.re.kr (S.E. Ryu).

tions of the TLN complexes formed with D-**1** and L-**2**, more potent enantiomers of **1** and **2**.



Results and Discussion

Chemistry

The synthetic route for inhibitor **1** is outlined in Scheme 1. The conversion of α -PheNHMe into **5** was carried out in one-pot following the general method reported by Feenstra et al.⁸ and the *N*-formylation of **5** to obtain **1** was performed by the method of Jahngen and Rosso-mando⁹ using the mixture of formic acid and acetic anhydride. The synthesis of **2** was reported previously.⁷

Inhibitory assay

The compounds were assayed as competitive inhibitors for TLN using *N*-[3-(2-furyl)acryloyl]Gly-Leu-NH₂¹⁰ as substrate at pH 7.2 and 25 °C. The inhibitory constants (K_i s) were obtained from the respective plot for v_o/v against the concentration of inhibitors and are presented in Table 1. Figure 1 exemplifies the plots. Inconsistent with the previous studies,^{6,7} the D-isomer was more potent than its enantiomer by 24-fold in the case of **1**, but in the inhibition with hydroxamate of β -PheNHMe, the L-isomer was more effective than the D-form by 41-fold. L-**2** is found to be more potent than D-**1** by 63-fold.

Crystal structures of TLN complexes formed with D-**1** and L-**2**

Crystals of the TLN-inhibitor complexes were obtained by soaking TLN crystals in a solution containing the inhibitor under study, and structures of the complexes were determined by using the structure of native TLN

Table 1. Inhibition of thermolysin

Inhibitor	K_i (μ M)
L- 1	2490 \pm 130
D- 1	104 \pm 4.8
L- 2	1.66 \pm 0.05 ^a
D- 2	68.2 \pm 5.6 ^a

^aRef 6.

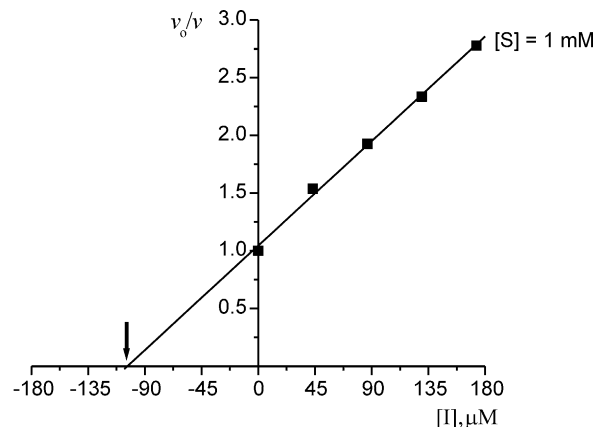
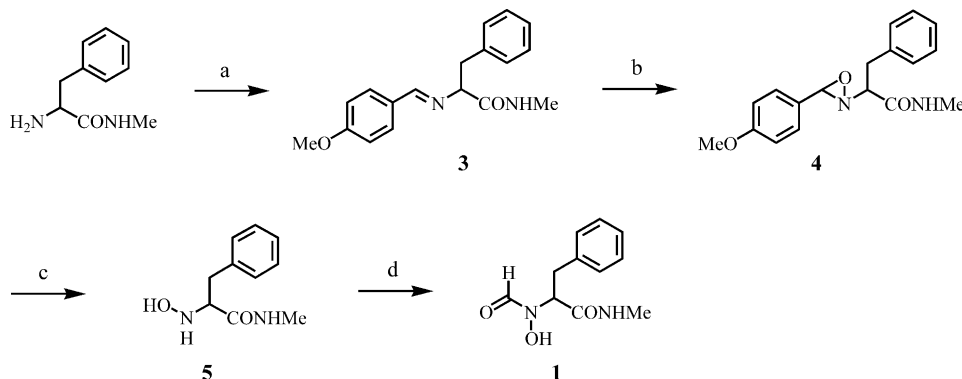


Figure 1. Determination of the K_i value for inhibition of TLN with D-**1**. In the plot the intercept of the straight line on $[I]$ would give the K_i value (see Experimental).

(pdb code:1LNF) as the starting model. The 2Fo-Fc map produced from the rigid-body refinement showed the overall feature of the bound inhibitors. In the case of TLN-L-**2** complex, subsequent refinement and rebuilding cycles produced well-defined structure for the bound inhibitor as well as the protein, but for TLN-D-**1** complex the electron density in the S₁' pocket was weak (see below). A summary of the crystallographic statistics is shown in Table 2.

The electron density map for the TLN-L-**2** complex (Fig. 2) clearly shows that one molecule of the inhibitor is bound to the active site of TLN. Both oxygen atoms of the hydroxamate moiety in L-**2** are involved in strong coordinative bondings to the active site zinc ion having bond distances of 2.00 and 2.36 Å. In addition, the formyl oxygen in the hydroxamate is engaged in hydrogen bonding with one of carboxylate oxygens of Glu-143, and the hydroxyl in the hydroxamate moiety is hydrogen



Scheme 1. Reagents, conditions, and yield: (a) *p*-anisaldehyde, MeOH, rt, 12 h, 91%; (b) *m*CPBA, CH₂Cl₂, rt, 12 h, quantitative; (c) HONH₂·HCl, MeOH, rt, 12 h, 71%; (d) (i) Ac₂O, HCO₂H, 0 °C, 2 h; (ii) 2 N NaOH, rt, 30 min, 56%.

Table 2. Crystallographic data

	TLN: L-2	TLN: D-1
Space group	P6 ₁ 22	P6 ₁ 22
Unit cell		
a, b, c (Å)	93.6, 93.6, 131.9	93.8, 93.8, 131.6
α, β, γ (°)	90.0, 90.0, 120.0	90.0, 90.0, 120.0
Resolution range (Å)	99–2.1	99–2.1
Number of unique reflections	18,917	19,725
Overall completeness (%)	91.8	95.6
R _{merge} (%) ^a	8.6	9.1
Number of atoms		
Protein atoms	2432	2432
Non-protein atoms	172	151
R _{cryst} (%) ^b	15.7	16.4
R _{free} (%) ^c	18.5	19.3
Rms deviations		
Bonds (Å)	0.006	0.005
Angles (°)	1.2	1.1
Dihedrals (°)	23.1	23.1
Improvers (°)	0.72	0.65

^aR_{merge} = $\sum_i |I_i - \langle I \rangle| / \sum_i \langle I \rangle$, where I is the intensity for the i th measurement of an equivalent reflection with the indices h, k, l .

^bR_{cryst} = $\sum |F_o - F_c| / \sum F_o$, where F_o and F_c are the observed and calculated structure factor amplitudes, respectively.

^cThe R_{free} value was calculated from 5% of all data that were not used in the refinement.

bonded to the imidazole NH of His-231. The benzene ring of L-2 is inserted in the S₁' hydrophobic pocket like that in substrate does. Important binding interactions between TLN and the bound inhibitors are listed in Table 3.

The electron density in the S₁' pocket for the TLN-D-1 complex (Fig. 3) is weak and significantly different from that in the complex of TLN-L-2. The electron density map in the S₁' pocket is best accounted for by a methylcarbamoyl moiety. The benzyl moiety of D-1 was not found in the refined electron density map, suggesting strongly that the side chain is exposed to the solvent region in a highly dynamic conformation. Thus, in the binding of D-1 to TLN, the benzyl and *N*-methylcarbamoyl moieties are interchanged compared with the binding of L-2 to TLN. Other regions of the inhibitor including the α-carbon and the hydroxamate moiety were well resolved. Both oxygen atoms of the hydroxamate bind to the active site zinc ion in a bidentate fashion with O–Zn distances of 2.11 and 2.63 Å. The formyl oxygen in D-1 is engaged in a hydrogen bonding with one of Glu-143 carboxylate oxygens, like that in L-2, and the aminohydroxyl oxygen is positioned within a hydrogen bonding distance to an imidazole ring nitrogen

Table 3. Selected bond distances (Å) in TLN-inhibitor complexes

Atoms in interactions ^a	TLN-D-1	TLN-L-2
TLN		
Inhibitor		
Zn ²⁺ ----- O ²	2.11	2.00
Zn ²⁺ ----- O ³	2.63	2.36
His ²³¹ -Im ⁻ ---- O ²	2.52	2.55
Glu ¹⁴³ -CO ₂ H ⁻ -- O ³	2.98	2.72
Arg ²⁰³ -GuaNH - O ¹	3.17	2.93
Asn ¹¹² -CONH -- N ¹	5.68	2.88
Tyr ¹⁵⁷ -OH ----- O ²	3.44	3.22

^aNumbering of inhibitor atoms is shown in the structure of the inhibitors.

atom of His-231. It may be inferred from the structures of the both complexes that the carboxylate of Glu-143 exists as a protonated form but the hydroxyl of the hydroxamate ligates the zinc ion in a deprotonated form. Cross et al. reported that upon binding of hydroxamate to a coordinated zinc ion such as that in the active site of zinc proteases, the pK_a of the ligand is attenuated markedly,¹¹ and Holmes and Matthews described that in the binding of L-LeuNH₂OH to TLN, the anionic form of the hydroxamate coordinates to the zinc ion.¹² In the binding of L-2 to TLN, the nitrogen and oxygen atoms of the methylcarbamoyl group are engaged in a hydrogen bond with the peptide carbonyl oxygen of Asn-112 and one of guanidinium nitrogens of Arg-203 of the enzyme, respectively (Table 3). On the other hand, the methylcarbamoyl group in D-1 just occupies the P₁' pocket without forming hydrogen bond with the enzyme. The difference in binding feature between D-1 and L-2 is illustrated in Figure 4.

Binding features of D-1 and L-2 to TLN are examined in an effort to understand the stereo-preference shown by the inhibitors in their inhibitions of TLN. In addition to the reversed stereo-preference shown in the binding of the two inhibitors, the α-carbon of D-1 is moved towards the zinc ion by about 0.6 Å compared with that of L-2, suggesting that in the bindings of the two inhibitors to TLN, the coordination of hydroxamate to the zinc ion plays a dominant role as expected from the strong coordination power⁵ of hydroxamate group to zinc ion. The much reduced binding affinity and the reversed stereospecificity in the complexing of 1 compared with those exhibited by 2 may be envisioned: because of the strong binding affinity of the hydroxamate towards the active site zinc ion, the α-carbon of 1 cannot rest at the locus where the α-carbon of substrate lies

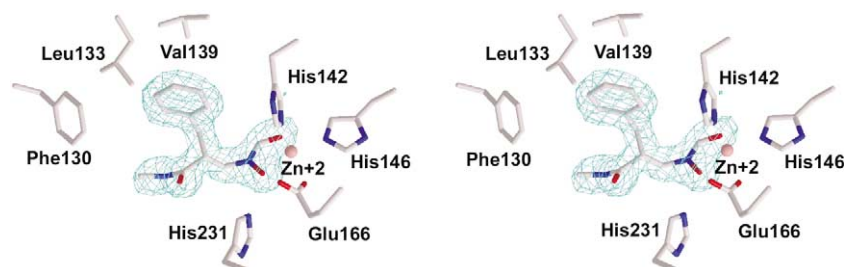


Figure 2. The difference electron density map for TLN-L-2 was generated with the final model omitting the bound inhibitor. The stereo map contoured at a 3.0 σ level was presented as superposed with the refined model.

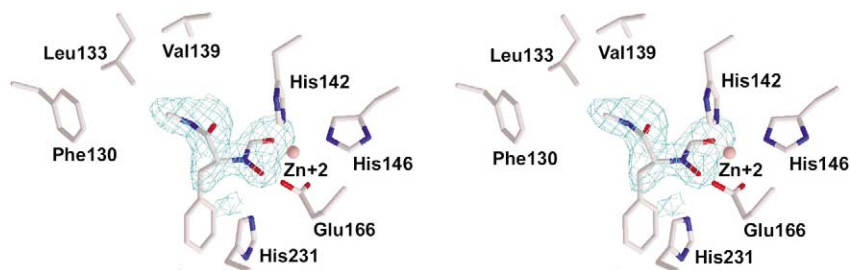


Figure 3. The difference electron density map for TLN-D-1 was generated with the final model omitting the bound inhibitor. The stereo map contoured at a 3.0σ level was presented as superposed with the refined model.

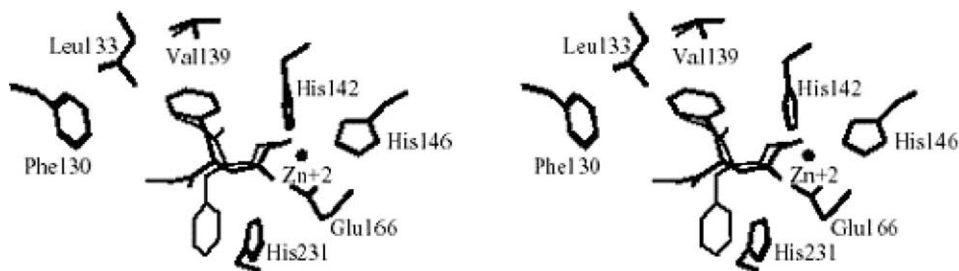


Figure 4. Superimposed stereoview of inhibitors D-1 and L-2 that are bound to TLN at the active site. Thin line represents D-1 and thick line denotes L-2.

upon its binding to TLN, and as a result the side chain phenyl ring in the P_1' residue of L-1 would difficultly rest in the S_1' pocket with difficulty, and thus L-1 shows much weaker binding affinity ($K_i = 2490 \pm 130 \mu\text{M}$). On the other hand, the relatively small methylcarbamoyl moiety of D-1 would be accommodated in the pocket, and D-1 exhibits a moderate binding affinity ($K_i = 104 \pm 4.8 \mu\text{M}$). In the case of **2** in which a methyl-ene unit is inserted between the hydroxamate moiety and the α -carbon of **1**, it is not unreasonable to assume that the hydroxamate hydroxyl is geometrically and functionally equivalent to the scissile amide carbonyl of substrate in view of the fact that the distance between the oxygen atom of the *N*-hydroxyl and the α -carbon in **2** is expected to be about the same as that between the carbonyl oxygen of P_1 residue and the α -carbon of P_1' residue in substrate. It is, therefore, expected that the side chain benzyl group of L-2 but not D-2 would rest at about the same region as the hydrophobic side chain of the P_1' residue in the substrate would when it forms complex with TLN. Accordingly, the aromatic ring of L-2 would be readily accommodated in the S_1' pocket when it binds TLN, and as a consequence L-2 binds and inhibits TLN much more strongly than its enantiomer.

Understanding of stereochemical effect of biologically active chiral compounds at the molecular level is of paramount importance, especially in connection with development of chiral drugs. In spite of its importance, our knowledge on the subject is very limited. The present study that unravels the stereochemical preference shown by the reversed hydroxamates of α - and β -PheNHMe would be of considerable value for designing small molecule inhibitors that are effective towards zinc proteases of etiological importance.

Experimental

Melting points were taken on a Thomas-Hoover capillary melting point apparatus and were uncorrected. ^1H NMR and ^{13}C NMR spectra were recorded with a Bruker AM 300 (300 MHz) instrument using tetramethylsilane as the internal standard. IR spectra were recorded on a Bruker Equinox 55 FT-IR spectrometer. Silica gel 60 (230–400 mesh) was used for flash chromatography and thin layer chromatography (TLC) was carried out on silica coated glass sheets (Merck silica gel 60 F-254). Elemental analyses were performed at Pohang University of Science and Technology, Pohang, Korea. Thermolysin (Type X) was purchased from Sigma Chemical Co. Solutions for kinetic study were prepared using doubly distilled and deionized water.

N-Hydroxy-L-phenylalanine methylamide (L-5)

To a solution of L-phenylalanine methylamide (1.77 g, 9.8 mmol) in anhydrous methanol (50 mL) was added *p*-methoxybenzaldehyde (1.3 mL, 10.8 mmol) and anhydrous Na_2CO_3 (1.6 g, 14.7 mmol). The mixture was stirred for 12 h under nitrogen atmosphere, then evaporated, and the residue was dissolved in ethyl acetate. The resulting solution was washed with water (50 mL \times 3), dried over anhydrous MgSO_4 , and concentrated under reduced pressure to give L-3 as a white solid (2.7 g, 91%). It was used without further purification for the preparation of L-4. Compound L-3 (2.7 g, 9.1 mmol) was dissolved in dry CH_2Cl_2 (100 mL) and cooled to 0°C . To this solution was added portionwise 3-chloroperoxybenzoic acid (over 77%, 2.2 g, 10 mmol) and stirred for 12 h at room temperature. The precipitated 3-chlorobenzoic acid was filtered off and the filtrate was washed with saturated NaHCO_3 solution (50 mL \times 3), brine (50 mL \times 3), dried over anhydrous

MgSO₄, and evaporated in vacuo to give oxaziridine L-4. Compound L-4 (2.8 g, 9.1 mmol) was dissolved in MeOH (100 mL) and to the resulting solution was added hydroxylamine hydrochloride (0.7 g, 10 mmol) was added. The mixture was stirred for 12 h at room temperature, then evaporated under reduced pressure. Water was added to the residue, and the mixture was washed with ether (50 mL × 3). The aqueous phase was neutralized with 5% NaHCO₃ solution and extracted with CH₂Cl₂ (50 mL × 3). The organic phase was dried over anhydrous MgSO₄, evaporated in vacuo, and the residue was recrystallized from methanol to afford L-5 as a white solid (1.25 g, 71%). Mp 152–154 °C (lit. 151–152.5 °C)⁷; $[\alpha]_{\text{D}}^{25} + 7.8^\circ$ (*c* 2, MeOH) (lit. $[\alpha]_{\text{D}}^{25} + 6.6^\circ$ (*c* 2, MeOH))⁷; ¹H NMR (CD₃OD, 300 MHz) δ 2.67 (s, 3H), 2.74–2.91 (m, 2H), 3.59 (t, 1H), 7.18–7.30 (m, 5H); ¹³C NMR (CD₃OD, 300 MHz) δ 25.0, 35.8, 68.4, 126.7, 128.5, 129.2, 137.7, 174.7. Anal. calcd for C₁₀H₁₄N₂O₂: C, 61.84; H, 7.27; N, 14.42. Found: C, 61.56; H, 7.23; N, 14.21.

N-Hydroxy-D-phenylalanine methylamide (D-5). Compound D-5 was prepared from D-phenylalanine methylamide in a manner analogous to that used for the preparation of L-5. $[\alpha]_{\text{D}}^{25} - 6.6^\circ$ (*c* 2, MeOH). Anal. calcd for C₁₀H₁₄N₂O₂: C, 61.84; H, 7.27; N, 14.42. Found: C, 61.58; H, 7.33; N, 14.24.

N-Hydroxy-N-formyl-L-phenylalanine methylamide (L-1). To the ice-chilled acetic anhydride (1 mL, 10.3 mmol) was added dropwise formic acid (95–97%, 0.5 mL, 12.8 mmol) and the resulting mixture was stirred for 5 min. The solution was heated at 50 °C for 5 min, then cooled to 0 °C. To the resulting solution was added L-5 (0.203 g, 1.04 mmol) at room temperature. The solution was stirred until L-5 was no longer detected when tested by TLC, concentrated, and the residue was dissolved in MeOH. The methanol solution was treated with 2 N NaOH, and evaporated under reduced pressure. The residue was treated with 3 N HCl. The aqueous solution was extracted with ether (50 mL × 3). The combined ether extracts were evaporated in vacuo and the solid residue that obtained was recrystallized from ethyl acetate to give L-1 as a white solid (0.13 g, 56%). Mp 169–169.5 °C. $[\alpha]_{\text{D}}^{25} + 7.6^\circ$ (*c* 0.5, MeOH). IR (CH₂Cl₂): 1664, 1735, 3324 cm⁻¹. ¹H NMR (DMSO-*d*₆, 300 MHz) δ 2.62 (d, 3H) 2.95–3.17 (m, 2H) 4.42 (dd, 1H) 4.89 (dd, 1H) 7.19–7.30 (m, 5H) 7.67 (s, 0.66H) 7.86 (d, 1H) 8.16 (s, 0.34H). ¹³C NMR (DMSO-*d*₆, 300 MHz) 26.7, 34.2 64.5 127.2 129.1 130.0 138.6 159.0 169.6. Anal. calcd for C₁₁H₁₄N₂O₃: C, 59.45; H, 6.35; N, 12.61. Found: C, 59.83; H, 6.23; N, 12.61.

N-Hydroxy-N-formyl-D-phenylalanine methylamide (D-1). Compound D-1 was prepared from D-5 in a manner analogous to that used for the preparation of L-1. $[\alpha]_{\text{D}}^{25} - 6.8^\circ$ (*c* 1, MeOH). Anal. calcd for C₁₁H₁₄N₂O₃: C, 59.45; H, 6.35; N, 12.61. Found: C, 59.26; H, 6.59; N, 12.76.

Determination of K_i value. Enzyme stock solution was prepared by dissolving TLN (3 mg) in 2 mL of pH 7.2 buffer 0.1 M Tris/0.01 M CaCl₂. Typically, the enzyme stock solution was added to a solution containing

FA-Gly-L-Leu-NH₂¹⁰ (final concentration, 1 mM) and inhibitor (four concentrations in the range of 0.04–4 mM) in 0.1 M Tris/0.01 M CaCl₂, pH 7.2 buffer (1 mL cuvette, the final content of DMF was controlled at 5%), and the change in absorbance at 345 nm was measured immediately. The final concentration of TLN was 0.45 μM. Initial velocities were then calculated from the initial linear portion of the change in absorbance where the amount of substrate consumed was less than 10%. The K_i values were determined from the plot of v_o/v against the concentration of inhibitors based on the equation, v_o/v = 1 + [I]/K_i in which v_o and v represent the initial velocity in the absence and presence of the inhibitor, respectively (Fig. 1). In the plot, the intercept of the straight on [I] would give the K_i value.

Crystal growth. TLN (Calbiochem) was crystallized as described by Holmes and Mathews¹³ with slight modifications. Briefly, TLN was dissolved in a 0.05 M Tris buffer (pH 7.2) solution containing DMSO [45% (v/v)] and calcium acetate (1.4 M) to have the final protein concentration of about 100 mg/mL. Crystals were grown by the hanging-drop vapor diffusion method by using a reservoir solution containing 0.01 M calcium acetate, 5% (v/v) DMSO and 0.05 M Tris buffer (pH 7.2). Native crystals of TLN were equilibrated in the reservoir solution supplemented with 10 mM of the inhibitor for 2–3 days to obtain crystals of TLN-inhibitor complex.

X-ray diffraction data collection and structure refinement. Diffraction data were collected by using a Rigaku RU300 rotating anode X-ray generator operating at 40 kV × 100 mA and R-axis IV++ imaging plate detector system. An R-axis data processing program (Rigaku) and the programs MOSFLM¹⁴ and SCALA¹⁵ were used for the data processing. After the initial rigid body refinement, several alternating cycles of model building and simulated annealing refinements were carried out. The programs O¹⁶ and CNS¹⁷ were used in the model building and refinement, respectively. The randomly selected 5% of the data were set aside for the R_{free} calculation. Water molecules were gradually added to the model with the waterpick routine in the program CNS. Although extra densities for the added inhibitors were apparent from the initial rigid body refinement stage, the inhibitor models were not included until the last stage of refinement.

Acknowledgements

The authors express their thanks to Ministry of Science and Technology and Korea Foundation for Science and Engineering for their financial supports of this work and Ministry of Education and Human Resources for the BK21 fellowship to JDP.

References and Notes

- (a) Matthews, B. W. *Acc. Chem. Res.* **1988**, *21*, 333. (b) Fersht, A. *Enzyme Structure and Mechanism*, 2nd ed.; W.H. Freeman & Co.: New York, 1977; p 418.

2. (a) Ondetti, M. A.; Rubin, B.; Cushman, D. W. *Science* **1977**, *196*, 441. (b) Cushman, D. W.; Cheung, H. S.; Sabo, E. F.; Ondetti, M. A. *Biochemistry* **1977**, *16*, 5484.
3. Whittaker, M.; Floyd, C. D.; Brown, P.; Gearing, A. J. H. *Chem. Rev.* **1999**, *99*, 2735.
4. Powers, J. C.; Harper, J. W. Inhibitors of Metalloproteases; In *Proteinase Inhibitors*, Barrett, A. J., Salvesen, G. Ed.; Elsevier: Amsterdam, 1986; pp 219–298.
5. Browner, M. F.; Smith, W. W.; Castelhana, A. L. *Biochemistry* **1995**, *34*, 6602.
6. Jin, Y.; Kim, D. H. *Tetrahedron: Asymmetry* **1997**, *8*, 3699.
7. Jin, Y.; Kim, D. H. *Bioorg. Med. Chem. Lett.* **1998**, *8*, 3515.
8. Feenstra, R. W.; Stokkingreef, E. H. M.; Reichenwein, A. M.; Lousberg, W. B. H.; Ottenheijm, H. C. J. *Tetrahedron* **1990**, *46*, 1745.
9. Jahngen, E. G. E.; Rossomando, E. F. *Syn. Commun.* **1982**, *12*, 601.
10. Feder, J. A. *Biochem. Biophys. Res. Commun.* **1968**, *32*, 326.
11. Cross, J. B.; Duca, J. S.; Kaminke, J. J.; Madison, V. S. *J. Am. Chem. Soc.* **2002**, *124*, 11004.
12. Holmes, M. A.; Matthews, B. W. *Biochemistry* **1981**, *20*, 6912.
13. Holmes, M. A.; Matthews, B. W. *J. Mol. Biol.* **1982**, *160*, 623.
14. Leslie, A. G. W. *Acta Crystallogr.* **1999**, *D55*, 1696.
15. Collaborative Computational Project Number 4 The CCP4 Suite: Programs for Protein Crystallography, *Acta Crystallogr.* **1994**, *D50*, 760.
16. Jones, T. A.; Zou, J. Y.; Cowan, S. W.; Kjeldgaard, M. *Acta Crystallogr.* **1991**, *A47*, 101.
17. Brünger, A. T.; Adams, P. D.; Clore, G. M.; DeLano, W. L.; Gros, P.; Grosse-Kunstleve, R. W.; Jiang, J. S.; Rice, L. M.; Simonson, T.; Warren, G. L. *Acta Crystallogr.* **1998**, *D54*, 905.